Carbohydrate Polymers 86 (2011) 147–153

Contents lists available at ScienceDirect

Carbohydrate Polymers

journal homepage: www.elsevier.com/locate/carbpol

Preservation of catechin antioxidant properties loaded in carbohydrate nanoparticles

Ivone Peres[a], Sandra Rocha[a,b], Joana Gomes[a], Simone Morais[c], M. Carmo Pereira[a], Manuel Coelho[a,*]

[a] LEPAE, Chemical Engineering Department, Faculty of Engineering, University of Porto, Rua Roberto Frias, 4200-465 Porto, Portugal
[b] Department of Radiation Biology, Institute for Cancer Research, Norwegian Radium Hospital, University Hospital, Montebello, 0310 Oslo, Norway
[c] REQUIMTE, Instituto Superior de Engenharia do Porto, Rua Dr. António Bernardino de Almeida 431, 4200-072 Porto, Portugal

ARTICLE INFO

Article history:
Received 27 January 2011
Received in revised form 20 March 2011
Accepted 12 April 2011
Available online 21 April 2011

Keywords:
Epigallocatechin gallate
Carbohydrates
Particles
Spray-drying
Polymeric drug carrier

ABSTRACT

Epigallocatechin gallate (EGCG), an antioxidant with several pharmacological and biological activities, was encapsulated in carbohydrate particles to preserve its antioxidant properties and improve its bioavailability. Gum arabic–maltodextrin particles loaded with EGCG (EGCG/P) were successfully produced by homogenization and spray-drying, with an EGCG loading efficiency of 96 ± 3%. Spray-dried particles are spherical or corrugated and polydisperse with diameters less than 20 μm. The particles in aqueous suspension revealed two main populations, with mean average diameters of 40 nm and 400 nm. Attenuated total reflection-infrared spectroscopy (ATR-IR) confirmed that EGCG was incorporated in the carbohydrate matrix by intermolecular interactions, maintaining its chemical integrity. Atomic force microscopy imaging proved the particle spherical shape and size. The present study demonstrates that the carbohydrate matrix is able to preserve EGCG antioxidant properties, as proof of concept to be used as polymeric drug carrier.

1. Introduction

Free radicals and oxidative stress are related to cancer, cardiovascular disease, diabetes, autoimmune disorders and neurological disorders (Warden, Smith, Beecher, Balentine, & Clevidence, 2001). Epidemiological studies have shown that a diet enriched in antioxidants is associated with reduced risk of such disorders (Ratnam, Ankola, Bhardwaj, Sahana, & Kumar, 2006). Antioxidants, such as catechins from green tea, show a wide range of biological activities including antithrombotic, vasodilatory and anticarcinogenic effects, as well as anti-inflammatory, antiallergic, antiulcer, and antimicrobial properties (Anand et al., 2008; Middleton, Kandaswami, & Theoharides, 2000). Catechins act as free radical scavengers and chelators of metal ions (Kandaswami & Middleton, 1994). Oral administration is the most efficient delivery system of antioxidants, however oral bioavailability of tea catechins is very low, less than 2–5% and their systemic clearance is also high (Cai, Anavy, & Chow, 2002; Dvorakova, Dorr, Valcic, Timmermann, & Alberts, 1999). Encapsulation of catechins in carbohydrate nanoparticles (Hu et al., 2008; Kosaraju, D'ath, & Lawrence, 2006), liposomes (Fang, Lee, Shen, & Huang, 2006) or other pre-formed materials (Shi et al., 2008), represents a solution to increase the antioxidant's efficacy of therapy. Spray-drying technology is widely used for drying biomolecules or colloidal particles and is based on a fast (~10 s) convective drying process, in which hot air provides energy for evaporation of solvent (water) from liquid drops formed by atomization (Masters, 1985). Mixtures of gum arabic and maltodextrin have shown promise as high solid carriers, giving acceptable viscosity in studies on microencapsulation of cardamom oil by spray-drying (Sankarikutty, Sreekumar, Narayanan, & Mathew, 1988). Gum arabic has good emulsifying capacity, low viscosity in aqueous solution and film forming properties, which aids the spray-drying process (Krishnan, Bhosale, & Singhal, 2005; Madene, Jacquot, Scher, & Desobry, 2006; Righetto & Netto, 2005). In addition, gum arabic is resistant to human endogenous enzymes and is completely digested by intestinal bacteria, followed by absorption (Phillips, Ogasawara, & Ushida, 2008). Maltodextrin is a good compromise between cost and effectiveness, as it is bland in flavour, has low viscosity at a high solid ratio and is available in different average molecular weights (Madene et al., 2006). The polysaccharide properties will determine the density and size of spray-dried particles (Elversson, Andersson, & Millqvist-Fureby, 2007; Elversson & Millqvist-Fureby, 2005). Depending on the molecule, either amorphous hollow or crystalline porous particles can be formed.

In this work, gum arabic–maltodextrin particles loaded with epigallocatechin gallate were produced by homogenization and spray-drying and their features were characterized in solid state and aqueous medium. Apparent density, true density and pore size distribution of spray-dried particles were obtained. The stabil-

* Corresponding author. Tel.: +351 225081679; fax: +351 225081449.
E-mail address: mcoelho@fe.up.pt (M. Coelho).

0144-8617/$ – see front matter © 2011 Elsevier Ltd. All rights reserved.
doi:10.1016/j.carbpol.2011.04.029

ity of EGCG incorporated in the carbohydrate matrix was studied by measuring its antioxidant activity, to assess the efficacy of the encapsulation method.

2. Materials and methods

2.1. Materials

Gum arabic (250 kDa) was purchased from Sigma–Aldrich Co. (USA). Maltodextrin (1000 Da) and catechins Sunphenon EGCG (458 Da) were kindly provided by Grain Processing Corporation (USA) and Taiyo Kaguku (Japan), respectively. All chemicals were used without further purification. The ultrapure water (resistivity of 18.2 MΩ cm) was obtained using an EasyPure RF purification system (Nanopure Diamond Water Purification, Barnstead Thermo Scientific, USA).

2.2. Preparation of carbohydrate particles

Gum arabic was dissolved in ultrapure water at 50–60 °C, adding the maltodextrin, in a proportion of 60 wt.%, under magnetic stirring for 30 min to form an aqueous suspension. The suspension was homogenized at a constant speed (9500 rpm) with a dispersing device IKA DI25 Basic (Staufen, Germany). The resultant suspension was fed to a spray-dryer (designed by Niro A/S) at the following conditions: inlet air temperature between 150 and 170 °C, outlet air temperature between 50 and 60 °C, and a liquid feed flow rate of 10 ml/min. The spray-dried powder was then collected to the spray-dryer's glass collecting vessel. The epigallocatechin gallate (EGCG) loaded particles (EGCG/P) were prepared following the same procedure but adding EGCG to the suspension before homogenization, in a proportion of 5 wt.%.

2.3. Characterization of carbohydrate particles

2.3.1. Scanning electron microscopy (SEM)

The surface morphology of the spray-dried EGCG/P was examined by means of a JEOL SEM 6301F microscope (Tokyo, Japan). The samples in solid state were previously fixed on a brass stub using double-sided adhesive tape. Then they were coated with a thin layer of platinum in vacuum to be electrically conductive. Micrographs were taken at an excitation voltage of 7 kV. Cryogenic scanning electron microscopy was used for particle characterization in aqueous suspension. Samples were frozen in liquid nitrogen, the temperature was raised slightly to sublime any condensed water off the surface of the sample, which was then coated with gold and observed under vacuum.

2.3.2. Zeta potential and Dynamic light scattering (DLS)

The zeta potential and the hydrodynamic diameter of EGCG/P were determined by laser doppler velocimetry and DLS, respectively, using a Zetasizer Nano ZS (Malvern Ltd, UK). Each sample was measured at two different concentrations (0.2 and 0.3 wt.%) in ultrapure water.

2.3.3. Atomic force microscopy (AFM)

EGCG/P shape and size were studied by AFM, using a JPK NanoWizard II BioAFM microscope (Berlin, Germany) assembled on a Carl ZEISS Axiovert 200 (biomaGUNE, San Sebastian, Spain). Standard glass cover slips of 0.17 mm thickness were washed with acetone and cleaned with tissue paper before being immersed in a 2% Hellmanex solution for 30 min. To decrease the negative charge density of the glass cover slips surface, they were coated with cationic PEI and rinsed with ultrapure water (0.01 M, NaCl 0.5 M). The substrates were then washed with ultrapure water and placed in a UV cleaner apparatus for 30 min. Afterward the substrate was incubated in a particle suspension (0.1 mg/ml) for 20 min and subsequently washed with water. The substrate was mounted into the cover slip holder with 500 μl of buffer solution. AFM imaging was obtained with unmodified silicon nitride tips (DNP, Veeco Instruments, USA) operating in intermittent contact mode. The nominal radius of curvature of the cantilevers was 20 nm and the spring constant of the cantilever, k_c, was calculated by the thermal method and corresponds to 336 ± 18 mN/m.

2.3.4. Helium pycnometry

Helium (He) displacement density, also called the true density, of EGCG/P was measured by He pycnometry employing Archimedes principle of fluid displacement and Boyle's law to determine the volume (Saravanapavan & Hench, 2003). The displaced fluid is a gas, which can penetrate the finest pores and thereby obtain maximum accuracy. Helium is usually used in these experiments as its small dimensions assure penetration into crevices and pores approaching one Angstrom (1 Å). Its behavior as an ideal gas is also desirable as the instrument uses the ideal gas equation to measure the volume occupied by the sample. The measurements were repeated at least three times.

2.3.5. Mercury porosimetry

Porosity parameters of EGCG/P such as pore size distribution, total surface area, average pore diameters and apparent density were evaluated by mercury (Hg) porosimetry, using a Quantachrome Poremaster (33/60). The low-pressure stations have a working pressure range of 0.5–50 psi (3.5–350 kPa) while the range for the high-pressure stations are between 20 and 60,000 psi (140 kPa–420 MPa). Hg porosimetry is based on the concept that the structure of porous solids can be characterized by forcing a non-wetting liquid to penetrate their pores (Saravanapavan & Hench, 2003). After evacuation, the cell is filled with Hg and then pressure is applied to force its entry into the sample pores. The amount of intruded Hg is related to the sample pore size and porosity.

2.3.6. Attenuated total reflection-infrared spectroscopy (ATR-IR)

ATR-IR spectra of EGCG/P and unloaded particles (control) were recorded employing a FTLA2000 Series Laboratory FT-IR Spectrometer (Ettlingen, Germany). The samples were analyzed in solid state and the spectra measured in a frequency range between 4000 and 450 cm^{-1}.

2.3.7. Microwave-assisted extraction (MAE)

MAE was used to determine the EGCG loading efficiency. MAE experiments were performed with a MARS-X 1500W Microwave Accelerated Reaction System for extraction and digestion (CEM Corp., Mathews, NC, USA). Samples of 10.0 mg of free EGCG, EGCG/P and control particles were suspended in 15 ml of methanol and transferred to the glass extraction vessels. Samples were extracted at two selected temperatures (90 and 110 °C), with constant medium stirring, at 100% magnetron power, for 15 min. The maximum vessel pressure cut off was set at 1.38×10^6 Pa. Once the extraction was completed, the samples were cooled for 10 min. The pellet (particles without EGCG) was discarded and the supernatant (extracted EGCG) analyzed by UV–VIS spectroscopy (UV-1700 PharmaSpec Spectrometer, Kyoto, Japan). The loading efficiency was determined according to the EGCG absorbance obtained at 276 nm. All experiments were performed, at least, in triplicate.

2.3.8. Radical scavenging capacity assay

Antioxidant activity of free EGCG, EGCG/P and control particles was determined according to the high-throughput relative 2,2,diphenyl-1-picrylhydrazyl radical (DPPH*) scavenging capacity assay (Cheng, Moore, & Yu, 2006) in a 96-well plate, using a Synergy™ 2 Multi-Detection Microplate Reader (BioTek

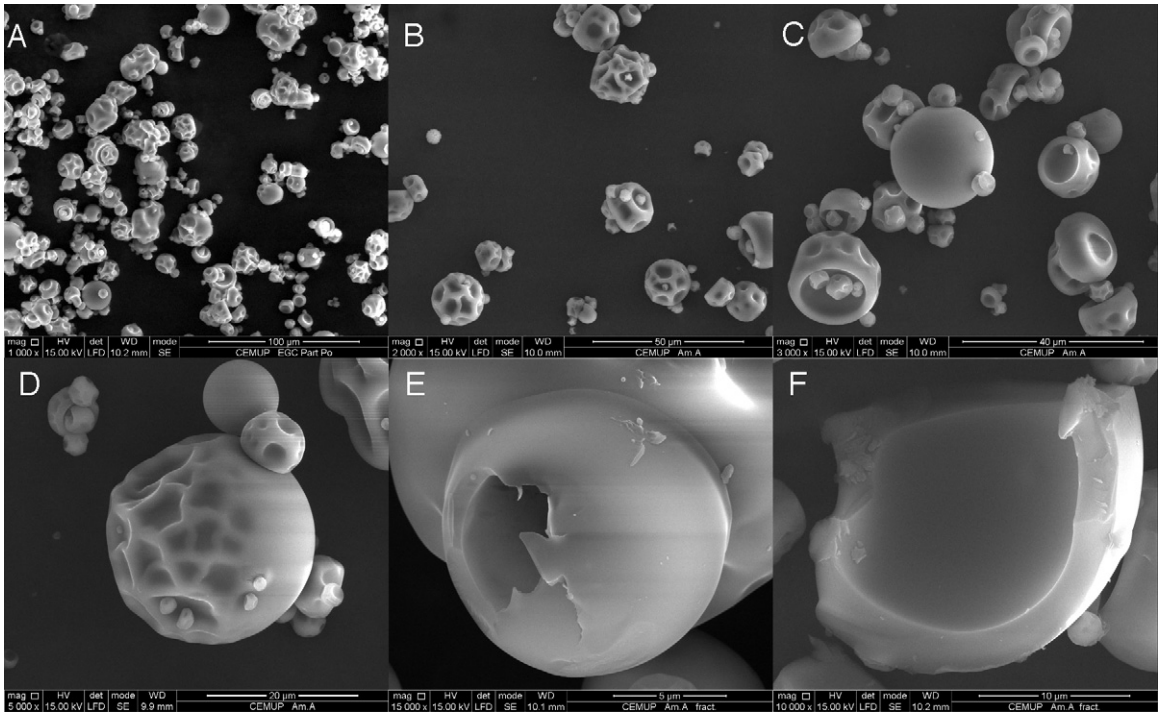

Fig. 1. Morphology of spray-dried EGCG/P. The particles on the bottom-right were intentionally crushed to show their internal structure. Scale bars represent 100 μm (A), 50 μm (B), 40 μm (C), 20 μm (D), 10 μm (E) and 5 μm (F).

Instruments, Vermont, USA). Five different EGCG concentrations, between 5.00 and 30.00 μM, were used for free EGCG and EGCG/P analysis. A sample of control particles was also analyzed. The assay was performed as follows: 100 μl of DPPH* methanol solution (0.208 mM) was added to 100 μl of sample into each well, using an eight channel micropipette followed by gentle shaking. The absorption was measured at 515 nm immediately after shaking and read once per minute for 90 min. A blank with the mixture of 100 μl water and 100 μl methanol, and a control with the mixture of 100 μl methanol and 100 μl DPPH* (0.208 mM) were also measured. The percentage of radical remaining at 40 min (%DPPH* remaining) was determined according to the following equation:

$$\%\mathrm{DPPH}^*_{\mathrm{remaining}} = \frac{A_{sample} - A_{blank}}{A_{control} - A_{blank}} \times 100 \quad (1)$$

where A_{sample}, A_{blank} and $A_{control}$ stand for the absorbance of sample, blank and control reactions at 40 min. To estimate the total DPPH* scavenging capacity of each sample, the percentage of DPPH* quenched (%DPPH* quenched) was determined according to the following equation:

$$\%\mathrm{DPPH}^*_{\mathrm{quenched}} = \left(1 - \frac{A_{sample} - A_{blank}}{A_{control} - A_{blank}}\right) \times 100 \quad (2)$$

where A_{sample}, A_{blank} and $A_{control}$, stand for the absorbance of the certain concentration of a selected sample, blank and the control at 515 nm measured at the reaction time *t*.

The values of %DPPH* quenched obtained from Eq. (2) were plotted against the reaction time and the value of the area under the curve (AUC) was determined. The aim of this method is to determine the relative DPPH* scavenging capacity (RDSC), expressed in trolox (standard antioxidant) equivalents (TE) per unit of testing material. Trolox demonstrated a linear relation between AUC and concentration changes with a correlation coefficient (r^2) of 0.9982. The RDSC values were determined, according to Eq. (3):

$$\mathrm{RDSC} = \frac{\mathrm{AUC}_{\mathrm{sample}}}{\mathrm{AUC}_{\mathrm{trolox}}} \times \frac{\mathrm{molarity}_{\mathrm{trolox}}}{\mathrm{molarity}_{\mathrm{sample}}} \quad (3)$$

The RDSC value was determined using a standard curve prepared with trolox at five concentrations within the linear range of 16–75 μM. Triplicate reactions were carried out for each concentration of antioxidant sample.

3. Results and discussion

3.1. Morphology of spray-dried particles

SEM micrographs of spray-dried particles show size polydispersity and diameters less than 20 μm (Fig. 1). The results depict structural differences between the particles. A population of disk-like and corrugated particles with highly dented surfaces is observed. Previous works demonstrated that spray-dried particles with wall materials consisting of polysaccharides exhibit notable surface indentation (Sheu & Rosenberg, 1998). On the other hand, Fig. 1 also reveals a particle population with spherical shape and smooth surface free of visible cracks and pores. Two intentionally crushed particles, shown in Fig. 1E and F, clearly demonstrate that the particles are hollow and have a dense shell.

The evaporation rate during spray drying is determined by the solute/solvent properties and processing parameters, predominantly air flow rate and temperature. The solidification mechanism, which depends on the nature of the component, is initiated once a critical concentration is reached at the surface (Vehring, 2008). The resulting particles will have different morphologies, depending on their size and the properties of their shells in the final stages of the drying process. Hollow spheres with smooth surface are formed, if the shell becomes rigid rapidly and does not buckle or fold (Vehring, 2008). The hollow particle may finally collapse or wrinkle (corrugate structure), depending on the thickness and mechanical properties of the shell. Also if the time to reach the

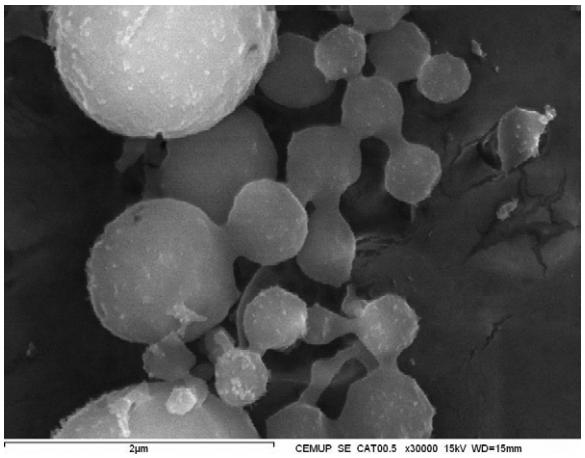

Fig. 2. Cryo-SEM micrograph of EGCG/P after re-suspension in ultrapure water. Scale bar represents 2 μm.

critical concentration for shell formation at the surface decreases, i.e. shell formation occurs earlier in the evaporation process on a larger droplet, particles with wrinkled surfaces are formed. It has been demonstrated that thermal expansion of air or water vapors inside the drying particles ("ballooning", associated with high drying rates) can smooth out dents (to a varying extent). The effectiveness of dent smoothing is dependent on the drying rate and on viscoelastic properties of the wall matrix (Rosenberg, Kopelman, & Talmon, 1985). Expansion and smoothing out of dents can occur only prior to solidification of the matrix when the wall matrix is elastic enough to enable such structural changes (Rosenberg et al., 1985). There are numerous examples in the literature reporting hollow and wrinkled or dimpled morphologies for spray-dried polymer particles (Baras, Benoit, & Gillard, 2000; Fu, Mi, Wong, & Shyu, 2001; Li & Birchall, 2006; Mu & Feng, 2001; Ting, Gonda, & Gipps, 1992; Wang & Wang, 2002). In addition, corrugated particles are typically produced by homogenization and spray-drying when using gum arabic as encapsulating agent (Rosenberg et al., 1985; Rosenberg, Talmon, & Kopelman, 1988).

Cryo-SEM analysis of the spray-dried EGCG/P dispersed in ultrapure water showed that corrugated particles disappeared and bridging of the particles occurred (Fig. 2).

DLS measurements of EGCG/P in suspension revealed a bimodal size distribution (Fig. 3A). The particle size distribution by intensity shows particles with mean diameters of 40 and 400 nm and a polydispersity index of 0.58 ± 0.06. The formation of small sized particle populations can be explained by the ion-dipole and hydrogen bond interactions between gum arabic and maltodextrin during homogenization.

The mean zeta potential of EGCG/P was -36 ± 6 mV, favoring the stability of the particle suspension (Fig. 3B).

AFM measurements confirm that the EGCG/P have a spherical shape (Fig. 4), similar diameters as found by DLS measurements (Fig. 3). Previous AFM studies concerning lipid coated carbohydrate particles demonstrated that polysaccharide core provides high resistance and mechanical strength (Gomes et al., 2010).

3.2. Particle internal structure/density

EGCG/P internal structure and density were studied by Hg porosimetry and He pycnometry. Fig. 5 shows usual patterns of the Hg porosimetry of EGCG/P. The dependence measured in Hg porosimetry is the pressure/volume relationship (Fig. 5A). Intrusion pressure values are directly converted into the corresponding pore size using the Washburn equation (Brabazon, Raffer, Waqar, & Mark, 2009). When mercury enters the pores of the sample, as

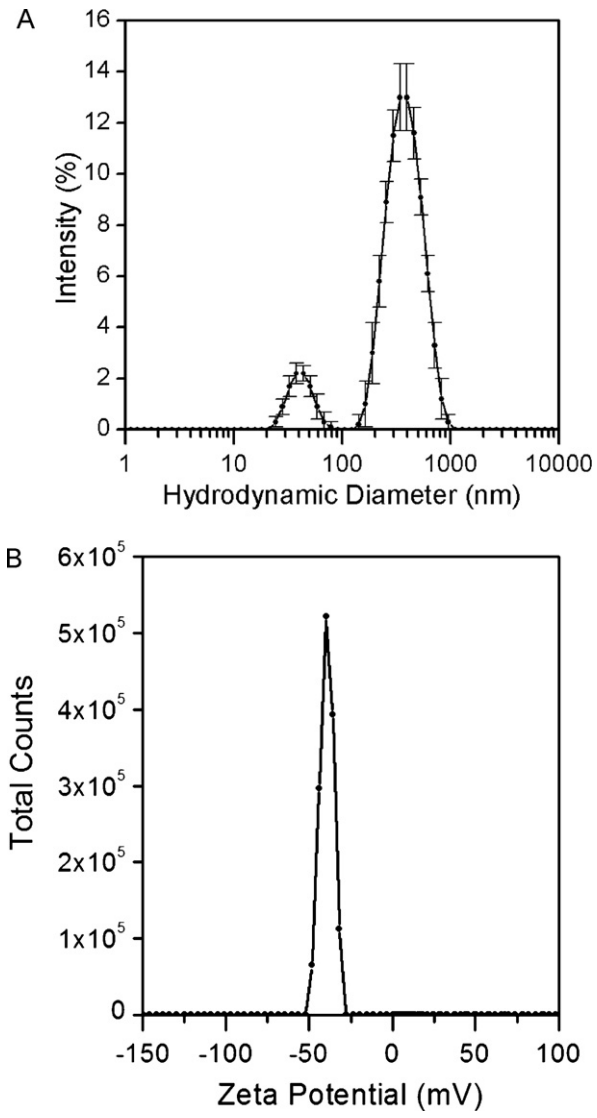

Fig. 3. Average hydrodynamic diameter distribution of EGCG/P (A) (average value ± standard deviation of 5 experiments) and zeta potential (B).

in the usual case, the pressure/volume relationship can be interpreted as distribution of pores. The pore size distribution is reported in Fig. 5B. The pore diameters range from 10 to 100 nm, with an average diameter of 24 nm. It is assumed that in high pressure porosimetry measurements – 20–60,000 psi (140 kPa–420 MPa), Hg fills all the cavities with a pore size between 3.5 nm and 900 μm, i.e. mesopores and macropores, whereas in He measurements, pores in diameter range of 0.1–300 nm (Alvarez & Borrego, 2005) are determined. The intraparticle porosity obtained from Hg porosimetry for EGCG/P was 0.2. Chemical composition of the particle surface such as an accumulation of polymeric material can change the permeability of the surface and hence the apparent particle density becomes less than the true density (Elversson et al., 2007; Elversson & Millqvist-Fureby, 2005).

Apparent density is the mass of a particle divided by its volume excluding open pores but including closed pores (that have not been penetrated by mercury at a pressure of 1 bar) (BS2955, 1958; Elversson et al., 2007). The apparent density determined from these data was 0.76 g/cm^3. Helium displacement density of EGCG/P was determined by He pycnometry – 1.36 g/cm^3. Unloaded particles revealed similar values of porosity and density. According to previous studies the apparent particle densities of the spray-dried

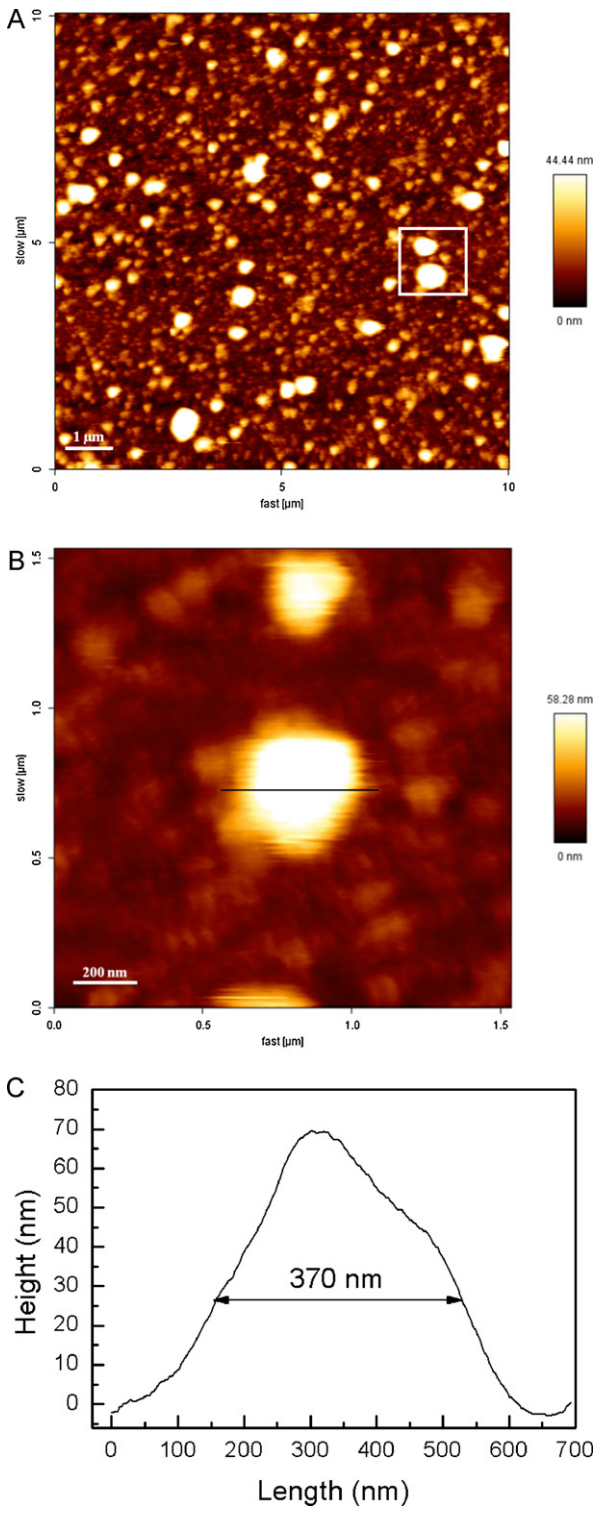

Fig. 4. AFM height images of EGCG/P. The signed area in image (A) was zoomed (B) to evidence the spherical shape of the particles. Scale bars represent 1 μm (A), 200 nm (B). The profile analysis of one particle is shown in image (C).

carbohydrates as determined by nitrogen pycnometry were negatively correlated to the concentration of the feed solution during spray drying: 1.54 g/cm^3, 1.45 g/cm^3 for lactose 5% and lactose 20% w/w, respectively; and 1.52 g/cm^3, 1.33 g/cm^3 for sucrose/dextran 20% w/w and sucrose/dextran 50% w/w, respectively. The apparent particle density of mannitol 15% w/w was 1.47 g/cm^3 (Elversson et al., 2007; Elversson & Millqvist-Fureby, 2005). Apparent particle densities close to the true density of the materials are correlated to either a network-like structure (porous solid) or completely gas permeable particles (Elversson & Millqvist-Fureby, 2005). In contrast, lower apparent densities seem to be related to hollow particle appearance, which is corroborated by our results (Fig. 1). Particle structure and density has been related to the crystallization propensity of carbohydrates. Hollow particles were shown to be formed by amorphous carbohydrates (e.g. lactose), whereas particles with network-like structure (porous solid) were more likely to be obtained from crystalline carbohydrates (e.g. mannitol) (Elversson et al., 2007; Vehring, 2008). Both gum arabic and maltodextrin are amorphous materials and film forming excipients (Swarbrick, 2006) thus prone to form hollow particles.

3.3. Loading efficiency

The loading efficiency was determined after MAE by measuring the total amount of EGCG in 10.0 mg sample of EGCG/P suspended in methanol, in which maltodextrin and gum arabic are insoluble. Methanol has a high dielectric constant, dipole moment and dissipation factor (the ability of a solvent to absorb microwave energy and pass it on in the form of heat to other molecules) (Eskilsson & Bjorklund, 2000) allowing appreciably superior recoveries than those obtained with other solvents (Perva-Uzunalic et al., 2006; Piñeiro, Palma, & Barroso, 2004). The EGCG quantification by UV–VIS spectroscopy revealed a loading efficiency of 92 ± 1% and 96 ± 3% at 90 °C and 110 °C, respectively. Accordingly with previous studies, higher recoveries of catechins using methanol as pressurized liquid solvent were attained at 110 °C (Eskilsson & Bjorklund, 2000; Piñeiro et al., 2004). Similarly to our results, EGCG encapsulation rate was nearly 100% in liposomes incorporated with ethanol (Fang et al., 2006). The main issues of using liposomes are related to the scaling up of the encapsulation process and to the delivery form of the liposome-encapsulated compounds. Usually, liposome formulations are kept in relatively dilute aqueous suspensions and this might be a very serious drawback for the large-scale production, storage, and shipping of encapsulated active compounds (Desai & Park, 2005). The entrapment efficiency of chitosan particles can vary from about 20% to 40–50%, depending mainly on the chitosan molecular weight and the proportion between chitosan and the ionic cross linker (sodium tripolyphosphate) (Hu et al., 2008; Zhang & Kosaraju, 2007). Chitosan is only soluble in acidic environment, which decreases the availability of catechins in the gastrointestinal tract.

ATR-IR spectrum of EGCG/P (Fig. 6) shows two absorption bands at 1560 cm^{-1} and 1475 cm^{-1}, not present in the spectrum of unloaded particles, which are attributed to C=C stretching of aromatic rings (Barras et al., 2009). The results confirm that EGCG molecules are incorporated in the carbohydrate matrix by intermolecular dipole–dipole interactions, since no chemical interaction was detected. In addition, this also indicates that EGCG chemical integrity was maintained after the spray-drying process. Previous studies on nuclear magnetic resonance spectroscopy (NMR) corroborate these findings, suggesting the entrapment of EGCG in the polysaccharide matrix (Peres et al., 2010).

3.4. Antioxidant activity of EGCG before and after spray-drying

Fig. 7 represents the values of DPPH* quenched at different EGCG concentrations for both free EGCG and EGCG/P samples.

EGCG and EGCG/P exhibit similar antioxidant activity for all concentrations tested, whereas the control particles, in the same mass concentration of EGCG/P, do not possess antioxidant activity (data not shown). RDSC values of free EGCG and EGCG/P at several concentrations are presented in Table 1.

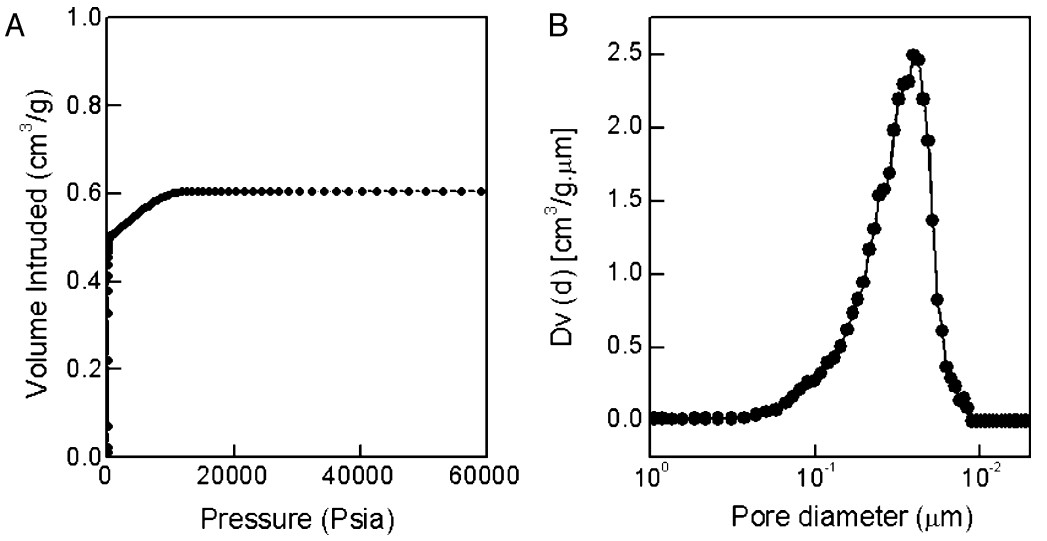

Fig. 5. Curves for EGCG/P obtained from Hg porosimetry: pressure/volume dependence (A) and pore size distribution (B).

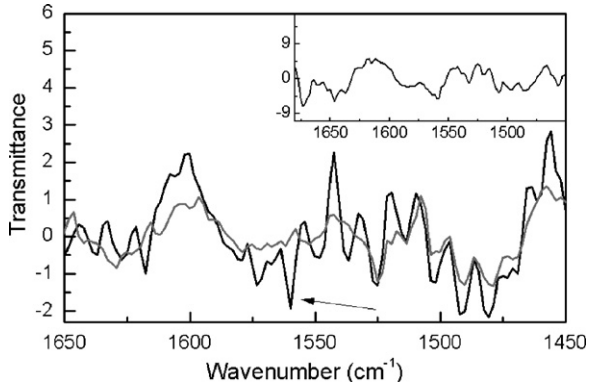

Fig. 6. ATR-IR spectra of EGCG/P (black line) and unloaded particles (gray line). The inset shows the spectrum of free EGCG.

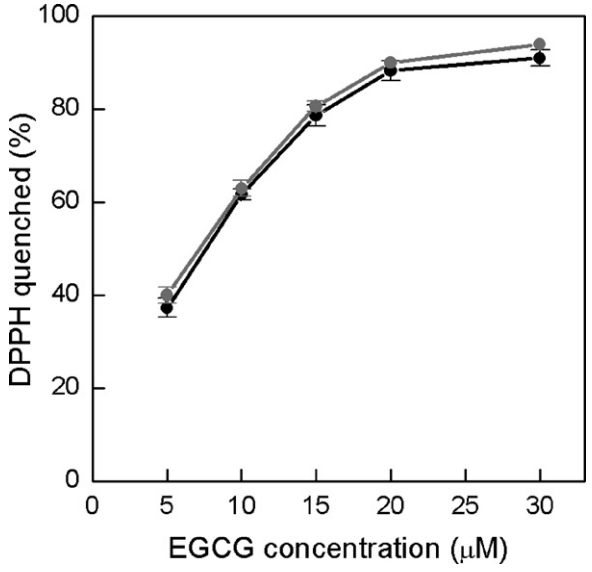

Fig. 7. Concentration effects of antioxidant-DPPH radical reactions for free EGCG (gray line) and EGCG/P (black line). Average value ± standard deviation, number of experiments = 3.

Table 1
Relative DPPH* scavenging capacity (RDSC) of free EGCG and EGCG/P at different concentrations.

Standard concentration (μM)	RDSC value (μM TE/μM)[a]	
	Free EGCG	EGCG/P
5.00	8.02 ± 0.37	7.48 ± 0.51
10.00	6.03 ± 0.10	6.12 ± 0.29
15.00	5.25 ± 0.06	5.37 ± 0.14
20.00	4.57 ± 0.08	4.62 ± 0.16
30.00	3.42 ± 0.01	3.34 ± 0.05

[a] Data correspond to the mean ± standard deviation of triplicate measurements.

RDSC is expressed in terms of trolox equivalents (TE) per unit of EGCG in order to compare the free radical scavenging capacities of antioxidants between different experiments and different testing times. In this study, the standard antioxidant used was trolox, because it can be dissolved in aqueous systems and in methanol. Trolox can be applied to report the relative radical scavenging capacities of both hydrophilic and lipophilic antioxidants, which allow to compare directly the DPPH* scavenging capacities of these antioxidants (Cheng et al., 2006). The study confirmed that EC_{50} values and RDSC determined at different concentrations are similar for both EGCG free and EGCG/P, which demonstrates that the loading method preserved the original antioxidant properties of the EGCG. The main objective of this study was to provide information about the antioxidant and radical scavenging potential of EGCG before and after incorporation in the carbohydrate matrix. The results obtained from these experiments demonstrated that free EGCG and EGCG/P manifested strong antioxidant and radical scavenging activities.

4. Conclusions

Our approach to the preservation of EGCG antioxidant properties is based on a carbohydrate particle formulation followed by spray-drying. The EGCG loading efficiency determined at the optimum extraction temperature (110 °C) was 96 ± 3%, which is a promising result for scaling up the process and pharmaceutical applications. The results confirmed the presence of EGCG within the carbohydrate matrix by intermolecular dipole–dipole interactions, maintaining its integrity after the spray-drying process. EGCG antioxidant activity was preserved even after the spray-drying process. The synthetic approach to the formulation of particles with the

capability to incorporate small to large-sized molecules in the carbohydrate matrix and simultaneously allowing the entrapment of other medium-sized molecules in the mesopores can be extended to other systems foreseeing chemical stabilization and protection from degradation in adverse conditions for pharmaceutical applications and, particularly, as drug delivery systems.

Recent studies highlight the use of polysaccharide nanoparticles in chemoprevention as they can be used to deliver natural antioxidants capable of inhibiting steps of the tumorigenesis process (Rocha et al., 2011; Siddiqui & Mukhtar, 2010).

Acknowledgements

This research is supported by grants from Agência de Inovação – Project BioCaps (QREN-European Union) and FCT (Science and Technology Foundation) – project PTDC\QUI-BIQ\102827\2008 and project PTDC/QUI-BIQ/115449/2009. Susana Moreno and José Toca-Herrera (Biosurfaces Unit, CIC BiomaGUNE, Spain) are gratefully acknowledged for AFM measurements.

References

Alvarez, D., & Borrego, A. G. (2005). Apparent versus true density for the volume-to-weight transformation in coal blends. *Journal of Microscopy-Oxford*, *220*, 221–228.

Anand, P., Kunnumakara, A. B., Sundaram, C., Harikumar, K. B., Tharakan, S. T., Lai, O. S., et al. (2008). Cancer is a preventable disease that requires major lifestyle changes. *Pharmaceutical Research*, *25*(9), 2097–2116.

Baras, B., Benoit, M. A., & Gillard, J. (2000). Parameters influencing the antigen release from spray-dried poly(DL-lactide) microparticles. *International Journal of Pharmaceutics*, *200*(1), 133–145.

Barras, A., Mezzetti, A., Richard, A., Lazzaroni, S., Roux, S., Melnyk, P., et al. (2009). Formulation and characterization of polyphenol-loaded lipid nanocapsules. *International Journal of Pharmaceutics*, *379*(2), 270–277.

Brabazon, D., Raffer, A., Waqar, A., & Mark, J. J. (2009). *Advanced characterization techniques for nanostructures. Emerging nanotechnologies for manufacturing*. Boston: William Andrew Publishing., pp. 59–91.

BS2955. (1958). *Glossary of terms relating to powders*. London: British Standards Institution.

Cai, Y., Anavy, N. D., & Chow, H. H. S. (2002). Contribution of presystemic hepatic extraction to the low oral bioavailability of green tea catechins in rats. *Drug Metabolism and Disposition*, *30*(11), 1246–1249.

Cheng, Z. H., Moore, J., & Yu, L. L. (2006). High-throughput relative DPPH radical scavenging capacity assay. *Journal of Agricultural and Food Chemistry*, *54*(20), 7429–7436.

Desai, K. G. H., & Park, H. J. (2005). Recent developments in microencapsulation of food ingredients. *Drying Technology*, *23*(7), 1361–1394.

Dvorakova, K., Dorr, R. T., Valcic, S., Timmermann, B., & Alberts, D. S. (1999). Pharmacokinetics of the green tea derivative, EGCG, by the topical route of administration in mouse and human skin. *Cancer Chemotherapy and Pharmacology*, *43*(4), 331–335.

Elversson, J., Andersson, K., & Millqvist-Fureby, A. (2007). An atomic force microscopy approach for assessment of particle density applied to single spray-dried carbohydrate particles. *Journal of Pharmaceutical Sciences*, *96*(4), 905–912.

Elversson, J., & Millqvist-Fureby, A. (2005). Particle size and density in spray drying – Effects of carbohydrate properties. *Journal of Pharmaceutical Sciences*, *94*(9), 2049–2060.

Eskilsson, C. S., & Bjorklund, E. (2000). Analytical-scale microwave-assisted extraction. *Journal of Chromatography A*, *902*(1), 227–250.

Fang, J. Y., Lee, W. R., Shen, S. C., & Huang, Y. L. (2006). Effect of liposome encapsulation of tea catechins on their accumulation in basal cell carcinomas. *Journal of Dermatological Science*, *42*(2), 101–109.

Fu, Y. J., Mi, F. L., Wong, T. B., & Shyu, S. S. (2001). Characteristic and controlled release of anticancer drug loaded poly (D,L-lactide) microparticles prepared by spray drying technique. *Journal of Microencapsulation*, *18*(6), 733–747.

Gomes, J. F. P. S., Rocha, S., Pereira, M. C., Peres, I., Moreno, S., Toca-Herrera, J., et al. (2010). Lipid/particle assemblies based on maltodextrin-gum arabic core as biocarriers. *Colloids and Surfaces B-Biointerfaces*, *76*(2), 449–455.

Hu, B., Pan, C. L., Sun, Y., Hou, Z. Y., Ye, H., Hu, B., et al. (2008). Optimization of fabrication parameters to produce chitosan-tripolyphosphate nanoparticles for delivery of tea catechins. *Journal of Agricultural and Food Chemistry*, *56*(16), 7451–7458.

Kandaswami, C., & Middleton, E. (1994). Free radical scavenging and antioxidant activity of plant flavonoids. *Free Radicals in Diagnostic Medicine*, *366*, 351–376.

Kosaraju, S. L., D'ath, L., & Lawrence, A. (2006). Preparation and characterisation of chitosan microspheres for antioxidant delivery. *Carbohydrate Polymers*, *64*(2), 163–167.

Krishnan, S., Bhosale, R., & Singhal, R. S. (2005). Microencapsulation of cardamom oleoresin: Evaluation of blends of gum arabic, maltodextrin and a modified starch as wall materials. *Carbohydrate Polymers*, *61*, 95–102.

Li, H. Y., & Birchall, J. (2006). Chitosan-modified dry powder formulations for pulmonary gene delivery. *Pharmaceutical Research*, *23*(5), 941–950.

Madene, A., Jacquot, M., Scher, J., & Desobry, S. (2006). Flavour encapsulation and controlled release – A review. *International Journal of Food Science and Technology*, *41*(1), 1–21.

Masters, K. (1985). *Spray drying handbook*. New York: John Wiley and Sons.

Middleton, E., Kandaswami, C., & Theoharides, T. C. (2000). The effects of plant flavonoids on mammalian cells: Implications for inflammation, heart disease, and cancer. *Pharmacological Reviews*, *52*(4), 673–751.

Mu, L., & Feng, S. S. (2001). Fabrication, characterization and in vitro release of paclitaxel (Taxol (R)) loaded poly (lactic-co-glycolic acid) microspheres prepared by spray drying technique with lipid/cholesterol emulsifiers. *Journal of Controlled Release*, *76*(3), 239–254.

Peres, I, Rocha, S., Pereira, M. C., Coelho, M. A. N., Rangel, M., & Ivanova, G. (2010). NMR structural analysis of epigallocatechin gallate loaded polysaccharide nanoparticles. *Carbohydrate Polymers*, *82*(3), 861–866.

Perva-Uzunalic, A., Skerget, M., Knez, Z., Weinreich, B., Otto, F., & Gruner, S. (2006). Extraction of active ingredients from green tea (*Camellia sinensis*): Extraction efficiency of major catechins and caffeine. *Food Chemistry*, *96*(4), 597–605.

Phillips, G. O., Ogasawara, T., & Ushida, K. (2008). The regulatory and scientific approach to defining gum arabic (*Acacia senegal* and *Acacia seyal*) as a dietary fibre. *Food Hydrocolloids*, *22*(1), 24–35.

Piñeiro, Z., Palma, M., & Barroso, C. G. (2004). Determination of catechins by means of extraction with pressurized liquids. *Journal of Chromatography A*, *1026*(1–2), 19–23.

Ratnam, D. V., Ankola, D. D., Bhardwaj, V., Sahana, D. K., & Kumar, M. N. V. R. (2006). Role of antioxidants in prophylaxis and therapy: A pharmaceutical perspective. *Journal of Controlled Release*, *113*, 189–207.

Righetto, A. M., & Netto, F. M. (2005). Effect of encapsulating materials on water sorption, glass transition and stability of juice from immature acerola. *International Journal of Food Properties*, *8*(2), 337–346.

Rocha, S., Generalov, R., Pereira, M. C., Peres, I., Juzenas, P., & Coelho, M. (2011). Epigallocatechin gallate-loaded polysaccharide nanoparticles for prostate cancer chemoprevention. *Nanomedicine*, *6*(1), 79–87.

Rosenberg, M., Kopelman, I. J., & Talmon, Y. (1985). A scanning electron microscopy study of microencapsulation. *Journal of Food Science*, *50*(1), 139–144.

Rosenberg, M., Talmon, Y., & Kopelman, I. J. (1988). The microstructure of spray-dried microcapsules. *Food Microstructure*, *7*(1), 15–23.

Sankarikutty, B., Sreekumar, M. M., Narayanan, C. S., & Mathew, A. G. (1988). Studies on microencapsulation of cardamom oil by spray drying technique. *Journal of Food Science and Technology-Mysore*, *25*(6), 352–356.

Saravanapavan, P., & Hench, L. L. (2003). Mesoporous calcium silicate glasses. II. Textural characterisation. *Journal of Non-Crystalline Solids*, *318*(1–2), 14–26.

Sheu, T. Y., & Rosenberg, M. (1998). Microstructure of microcapsules consisting of whey proteins and carbohydrates. *Journal of Food Science*, *63*(3), 491–494.

Shi, G. R., Rao, L. Q., Yu, H. Z., Xiang, H., Yang, H., & Ji, R. (2008). Stabilization and encapsulation of photosensitive resveratrol within yeast cell. *International Journal of Pharmaceutics*, *349*(1–2), 83–93.

Siddiqui, I. A., & Mukhtar, H. (2010). Nanochemoprevention by bioactive food components: A perspective. *Pharmaceutical Research*, *27*(6), 1054–1060.

Swarbrick, J. (2006). *Encyclopedia of pharmaceutical technology*. Taylor & Francis Group.

Ting, T. Y., Gonda, I., & Gipps, E. M. (1992). Microparticles of polyvinyl-alcohol for nasal delivery. 1. Generation by spray-drying and spray-desolvation. *Pharmaceutical Research*, *9*(10), 1330–1335.

Vehring, R. (2008). Pharmaceutical particle engineering via spray drying. *Pharmaceutical Research*, *25*(5), 999–1022.

Wang, F.-J., & Wang, C.-H. (2002). Sustained release of etanidazole from spray dried microspheres prepared by non-halogenated solvents. *Journal of Controlled Release*, *81*(3), 263–280.

Warden, B. A., Smith, L. S., Beecher, G. R., Balentine, D. A., & Clevidence, B. A. (2001). Catechins are bioavailable in men and women drinking black tea throughout the day. *The Journal of Nutrition*, *131*, 1731–1737.

Zhang, L. Y., & Kosaraju, S. L. (2007). Biopolymeric delivery system for controlled release of polyphenolic antioxidants. *European Polymer Journal*, *43*(7), 2956–2966.